EXPERIMENTAL INVESTIGATION ON THE SELF-PRESERVING BEHAVIOUR OF A TURBULENT PLANE JET WITH CO-FLOW

Jean Youssef
Cemagref
Université Européenne de Bretagne
17 avenue de Cucillé, F-35044 Rennes, France
jean.youssef@cemagref.fr

Johan Carlier
Cemagref
Université Européenne de Bretagne
17 avenue de Cucillé, F-35044 Rennes, France
johan.carlier@cemagref.fr

Joël Delville
Institut PPRIME,
CNRS-Université de Poitiers-ENSMA,
UPR 3346, CEAT F-86036 Poitiers, France
joel.delville@univ-poitiers.fr

Éva Dorignac
Institut PPRIME,
CNRS-Université de Poitiers-ENSMA,
UPR 3346, CEAT F-86036 Poitiers, France
eva.dorignac@univ-poitiers.fr

ABSTRACT

Air curtains are often used because of their ability to limit transfers between two atmospheres without the use of physical barrier. A typical air curtain is reproduced in a wind tunnel as a submerged plane jet in a uniform co-flow. This flow is explored by crossed Hot-Wire Anemometry for different Reynolds numbers and velocity ratios. The influence of these control parameters on the self-similar behaviours is discussed.

INTRODUCTION

A turbulent plane jet has several industrial applications, particularly in limiting transfer between two atmospheres without physical barriers (for example air curtains in tunnels and refrigerated cabinets). Depending on the application, the turbulent plane jet can be formed by various nozzle geometries ejecting into the same or different fluids. It can be warmed or cooled and pass successively forced, mixed and natural convection regimes. It can be semi-confined like wall or impinging jets. We aim to study the effect of plane jet between two parallel streams with different velocities and temperatures in the mixing layer. As prior study, we present in this paper an experimental investigation of a turbulent plane jet discharging into a simple parallel moving airstream at the same temperature.

A plane jet is defined as a statistically two-dimensional flow, with the dominant flow in the streamwise (x) direction, spreading in the lateral (y) direction and zero entrainment in the spanwise (z) direction. The turbulent plane jet discharging into a quiescent atmosphere was first studied by Van Der Hegge Zijnen (1958), Heskestad (1965) and Gutmark & Wygnanski (1976) and a similar jet discharging into an uniform co-flow was studied by Bradbury (1965), Everitt & Robins (1978) and Le Ribault *et al.* (1999). The former is referred to as a self-preserving pure jet type of flow. The latter can exhibit a self preserving structure in two limited regions of the flow. First, a self-preserving flow is possible when the velocity on the jet centreline is much greater than the free stream. This strong jet is referred to as the self-preserving pure jet type of flow. The second region in which a self-preserving flow is possible is when the jet centreline velocity is approaching the free stream velocity. This weak jet is a self-preserving wake flow type. Rajaratnam (1976) shows that for a strong jet ($\left(\langle u \rangle_{cl} - U_e\right)/U_e \gg 1$ with $\langle u \rangle_{cl}$, the mean velocity on the centreline and U_e, the co-flow velocity), the mean velocity on the centreline decreases as $x^{-1/2}$ and the width of the jet increases linearly. For a weak jet ($0 \leq \left(\langle u \rangle_{cl} - U_e\right)/U_e \ll 1$), the mean velocity on the centreline still decreases as $x^{-1/2}$, but the width of the jet increases as $x^{1/2}$. A plane jet discharging into a quiescent atmosphere always behaves as a strong jet whereas a plane jet with co-flow can behave as a strong jet near the exit and, due to the decrease of the mean velocity on the centreline, behaves as a weak jet farther downstream. The results in the literature do not show a clear behaviour of the constants (rate and virtual origin) involved in these self-similarity functions according to the Reynolds number Re and the velocity ratio r.

In this paper, the turbulent plane jet discharging into an uniform co-flow is explored by HWA (Hot-Wire Anemometry) in the region $0 \leq x/H < 37.5$, with H the jet width at the exit, for various control parameters (Re, r). This region includes the potential core, the transitional region and the self-similar region in which the turbulence is fully developed. The main objective is to determine the influence of these control parameters on the self-similar behaviour in the fully turbulent region.

EXPERIMENTAL SET UP

Besides the industrial and research interests of this flow configuration, the presence of the co-flow has numerous advantages for the experimental study of the jet. Temperature stratification and large convective motions are suppressed to prevent any perturbation in the jet development. There is no evenly back-mixing flow at the interface of the jet which allows HWA measurements. The flow can be homogeneously seeded everywhere to increase the quality of PIV (Particle Image Velocimetry) measurements. Moreover, a slight co-flow is often added in numerical simulations (see Le Ribault *et al.* (1999)) to avoid numerical difficulties. In this study, experiments consist in taking measurements by HWA for different configurations defined by a Reynolds number and a velocity ratio. HWA measurements are done in a specifically designed wind tunnel with lab-made constant temperature anemometers and crossed wires probes. This section described the wind tunnel and the HWA system and summarizes the characteristics of the different experiments.

Wind Tunnel

The wind tunnel was specifically designed for the experimental study of a plane jet in different configurations. This tunnel measures 5m high and has a section of $2 \times 2\text{m}^2$ in its basic configuration, the plane jet discharging into a parallel moving airstream. This tunnel is made up of three vertical and adjacent open-circuits. Each circuit has a centrifugal blower which supplies air to a plenum chamber followed by a convergent. The three plenum chambers are furnished with foams, honeycombs and screens to make the flow uniform with a low free stream turbulence intensity. For the central circuit, the plenum chamber measures $200 \times 20\text{cm}^2$ and the convergent has a contraction coefficient of 4. For the two adjacent circuits, the plenum chamber measures $200 \times 80\text{cm}^2$ and the asymmetrical convergent has a contraction coefficient of $8/6$. The flow discharging into the test section is a vertical plane jet of 4.8cm width and 200cm length between two uniform flows of 60cm width and 200cm length. The test section height is 200cm. The two walls parallel to the plane jet are porous screens to prevent confinement effects. The two end walls are in glass to allow optical diagnostic methods. The flow impacts the ground 50cm after the test section and naturally escapes on the sides. The flow velocity can be chosen continuously and independently between 1 and 12m/s for the plane jet and 0.3 and 2m/s for the co-flows. The plane jet temperature is controlled with air-water heat-exchanger located at the blower inlet. The co-flow temperature is adjusted by air conditioner of the hall. The origin of the axis (x,y,z) is located at the middle of the two trailing edge of separator plates. In this configuration, the mean velocity profile at the exit is shaped as a top hat with free stream turbulence intensity below 1%. The boundary layer over the separator plates are tripped downstream in order to fix the turbulence state and the onset of the transition. On the ouside plates, the boundary layer momentum thickness are about 3mm with a shape factor around 1.3 as expected for the turbulence state. On the inside, the boundary layers are too thin to allow significant measurements.

Hot-Wire Anemometry

Constant temperature anemometers with crossed hot-wires have been used for simultaneously measuring two velocity components in the plane defined by the wires. The anemometers were developed at CEAT (Centre d'Études Aérodynamiques et Thermiques, University of Poitiers) from TSI 1750 anemometers. Two lab-made miniature probes with crossed hot-wires were used to measure simultaneously the velocity components u and v for the first one and u and w for the second one. The wires were in platinum-plated tungsten with a diameter of 2.5µm, a length of 0.5mm and the angle between wires was about of 90°. The temperature measurement was performed with a type T thermocouple. The simultaneous recording of analogue signal was performed with an ETEP data acquisition system with integrated low-pass filters. Hot-wires probes and thermocouples were mounted on a profiled rake. The rake was fixed on one axis rotating system in a wind tunnel calibration for the calibration step and on three axis linear moving system for the measurement step in the plane jet wind tunnel.

The temperature regulation system provides the same temperature in the three fluxes. Nevertheless, this temperature may vary slightly (few tenths of degree) during an experiment or from one experiment to another. It is therefore necessary to calibrate the probes in temperature in addition to velocity and angle. The calibration law used is a system of 2 third order polynomial functions:

$$\|\vec{u}(t)\| = \sum_{i=0,j=0}^{i+j\leq 3} p_{ij}(e_1^{**})^i(e_2^{**})^j \tag{1}$$

$$\alpha(t) = \sum_{i=0,j=0}^{i+j\leq 3} q_{ij}(e_1^{**})^i(e_2^{**})^j \tag{2}$$

The main advantages of a such system are the explicit formulation for fast computing and the large velocity range of validity. This formulation links the norm $\|\vec{u}\|$ and the angle α of the velocity vector at the voltage e_1^{**} and e_2^{**}. The double asterisk denotes a temperature and drift compensation of the output voltage e measured across the anemometer. The temperature compensation is modeled by:

$$e_k^{*2}(t) = e_k{}^2(t)\left[\frac{\theta_k^w - \theta_o}{\theta_k^w - \theta(t)}\right] \tag{3}$$

where θ_k^w is the wire temperature and θ_o is any reference temperature. The drift compensation is defined as :

$$e_k^{**2}(t) = \frac{e_k^{*2}(t) - \left(a_{ok} + a_k'\right)}{\left(1 + b_k'\right)} \tag{4}$$

The coefficients a_{ok}, a_k' and b_k' come from the King's law $e_k^{*2} = a_k + b_k \cdot u_c{}^{n_k}$ where u_c is the cold velocity, $a_k = a_{ok} + a'_k$ and $b_k = (1 + b'_k)\, b_{ok}$.

The coefficients p_{ij}, q_{ij}, a_k and b_k and the exponents n_k are determined by calibration in a wind tunnel dedicated to the calibration of our sensors. The coefficients a'_k and b'_k related to the drift compensation are initially set to zero. They are regularly recomputed during the experimental campaign *in situ*, namely in the plane jet wind tunnel.

The calibration wind tunnel is a semi closed-loop wind tunnel. The test section has a length of 200cm and a square section of $28 \times 28\text{cm}^2$. The velocity profile at the entrance

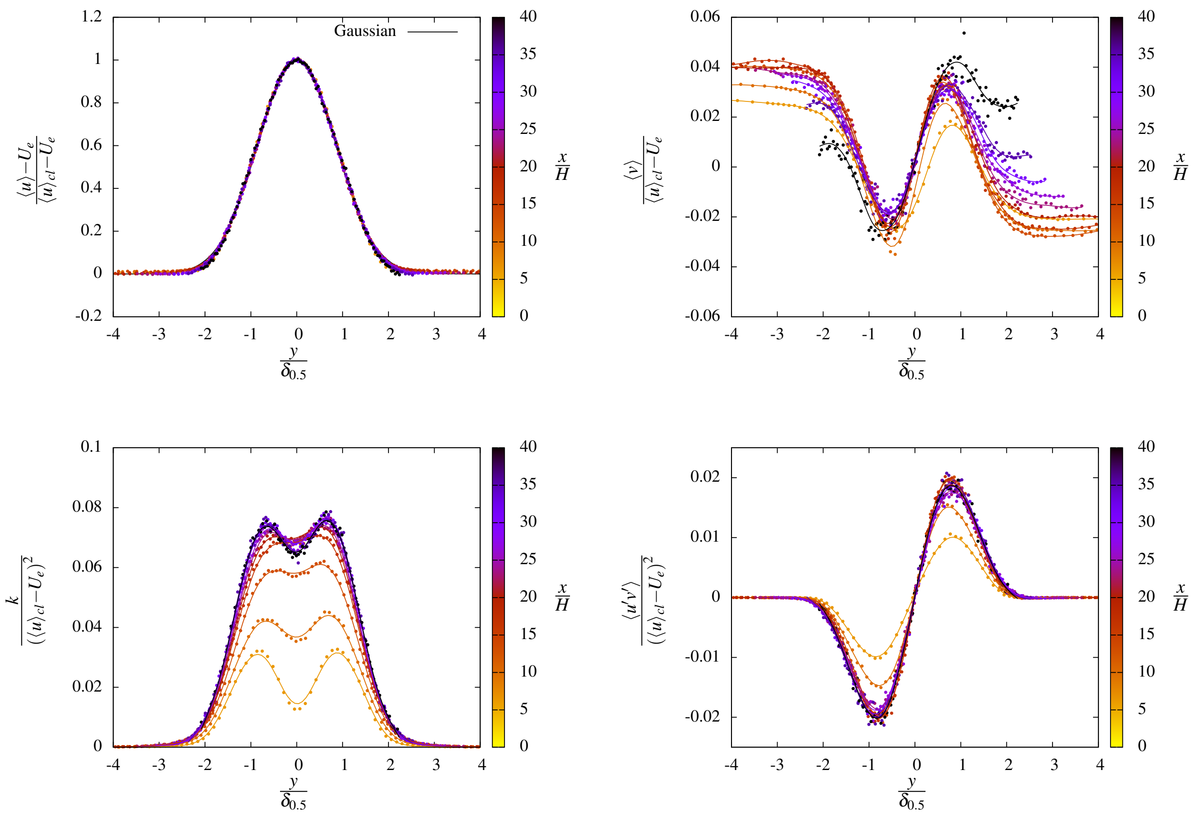

Figure 1. Normalized profiles of the main statistical quantities for $Re = 30{,}000$ and $r = 0.15$: top-left, mean velocity $\langle u \rangle$; top-right, mean velocity $\langle v \rangle$; bottom-left, mean turbulent kinematic energy $k = \frac{1}{2}\left(\langle u'u' \rangle + \langle v'v' \rangle + \langle w'w' \rangle\right)$; bottom-right, Reynolds shear stress $\langle u'v' \rangle$.

is uniform with a free stream turbulence intensity below 1%. A centrifugal blower supplies air to the test section with an adjustable velocity ranging from 0.5 to 12m/s. The temperature of the flow is controlled by an air-water heat-exchanger located at the blower inlet. This temperature can be varied between 5 and 40°C. The reference velocity u_r is deduced from the blower rotational speed previously calibrated by PIV. The reference temperature θ_r is given by a type T thermocouple.

The calibration procedure is done in two steps. The first step is the linear calibration of the probe (at zero incidence) where the output voltage is related to the cooling velocity and flow temperature using King's law. The flow velocity was varied following a sawtooth mode while the flow temperature was continuously decreased with a lower change rate to provide an equiprobable distribution of $(\|\vec{u}\|, \theta)$. The coefficients a_k and b_k, the exponents n_k and the wire temperatures θ_k^w (with ${a'}_k = 0$ and ${b'}_k = 0$) could be determined in a short single calibration run. The second step is the angular calibration where the norm and the angle velocity vector are related to the drift and temperature compensated voltage using eqns 1 and 2. For 13 angles α ranging from $-30°$ to $+30°$, the flow velocity was varied following a sawtooth mode while the flow temperature was constant. The p_{ij} and q_{ij} coefficients could be deduced from least-squares fit. The advantage of this procedure is that the p_{ij} and q_{ij} coefficients, determined in a dedicated wind tunnel, depend only on geometrical characteristics of the probe and has practically no drift while the linear calibration is come out *in-situ* and can easily be re-calibrated when a drift is observed.

Experiments

A plane jet discharging into a parallel moving airstream is defined by a Reynolds number $Re = \frac{(U_j - U_e)H}{\nu}$ and a velocity ratio $r = \frac{U_e}{U_j}$ where U_e is the co-flow velocity, U_j and H are the velocity and the width of the jet at the exit and ν is the kinematic viscosity. Far downstream from the origin, the mean behaviour of the jet becomes independent of the initial conditions (nozzle geometry, velocity profile, boundary layer) and depends only on the jet momentum thickness J and volume flow rate Q at the exit. For any form of mean velocity profile at the exit, U_j and H can be defined as:

$$J = \int_{-\infty}^{+\infty} \langle u \rangle \left(\langle u \rangle - U_e\right) dy = U_j \left(U_j - U_e\right) H \qquad (5)$$

$$Q = \int_{-\infty}^{+\infty} \left(\langle u \rangle - U_e\right) dy = \left(U_j - U_e\right) H \qquad (6)$$

where $\langle \cdot \rangle$ denotes the temporal average operator. In the present work, the mean velocity profiles at the exit is a "top-hat" function of height U_j and width H.

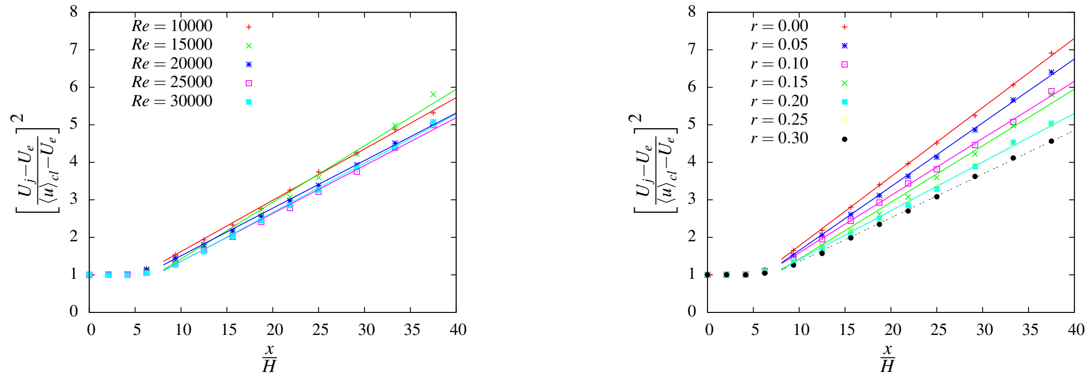

Figure 2. Mean velocity decay of $\langle u \rangle$ on the centreline: left, $r = 0.15$ for various Reynold numbers; right, $Re = 15,000$ for various velocity ratios. Lines are the fitting eqn 8 to the data.

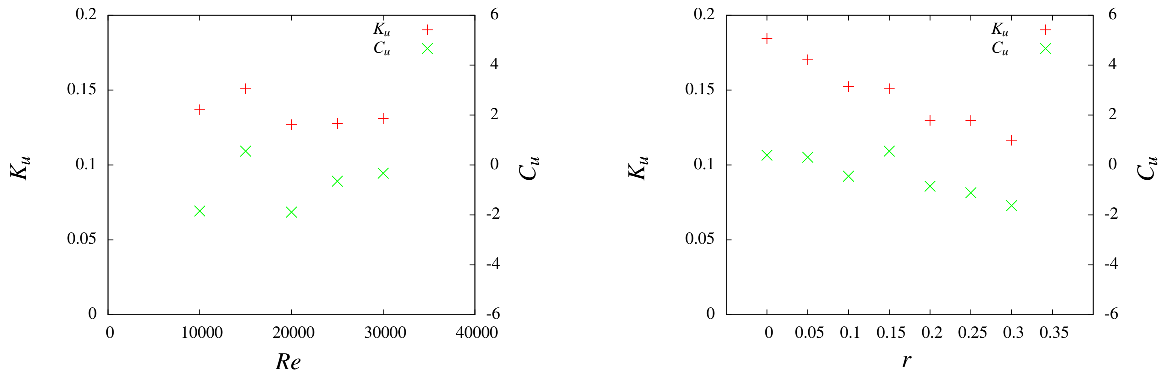

Figure 3. Centreline decay rate K_u and virtual origin C_u of the mean velocity: left, $r = 0.15$ for various Reynold numbers; right, $Re = 15,000$ for various velocity ratios.

To characterize the influence of the two control parameters on the behaviour of this flow, several configurations were explored. The velocity ratio is set at $r = 0.15$ for 5 Reynolds numbers ($Re = 10,000$, $15,000$, $20,000$, $25,000$ and $30,000$) and the Reynolds number is set at $Re = 15,000$ for 7 velocity ratios ($r = 0.00$, 0.05, 0.10, 0.15, 0.20, 0.25 and 0.30). With the jet width $H = 4.8$cm and the kinematic viscosity $\nu = 15 \cdot 10^{-6}\text{m}^2/\text{s}$, the jet and co-flow velocity ranges are $0 \leq U_e \leq 2$m/s and $3.8 \leq U_j \leq 11.5$m/s. One experiment consisted of measuring in the central plane of the jet $z = 0$ (z is an homogeneous direction) 13 velocity profiles (ranging from $x/H = 0$ to 37.5) with 101 points, *ie* $1,313$ points. The acquisition frequency was $12,500$Hz, the cutoff frequency of the anti-aliasing filter was $6,250$Hz and the number of acquisitions per point was $500,000$, given an acquisition time per point of 40s. These values can be related to the shedding frequency of the order of 10Hz in the experiments. The total duration of an experiment (acquisition and probe displacement) is about 20h.

RESULTS

The jet width H is given by the distance between the two separator plates. The jet velocity U_j and the co-flow velocity U_e are extracted from the mean velocity profiles at the jet exit which are shaped as a top-hat function. The centreline mean velocity jet $\langle u \rangle_{cl}$ and the velocity width of the jet δ are estimated by fitting a Gaussian function to the mean velocity profiles in the fully turbulent region (typically $\frac{x}{H} \geq 8$). This Gaussian function is expressed as:

$$\frac{\langle u \rangle - U_e}{\langle u \rangle_{cl} - U_e} = \exp\left[-\ln(\xi)\left(\frac{y}{\delta_\xi}\right)^2\right] \qquad (7)$$

with $\xi = 0.5$ to define the velocity half-width of the jet $\delta_{0.5}$ as the y value for which $\frac{\langle u \rangle - U_e}{\langle u \rangle_{cl} - U_e} = 0.5$. Particular attention was paid to the estimation of these characteristic quantities (H, U_j, U_e, $\langle u \rangle_{cl}$ and $\delta_{0.5}$) that express the overall behaviour of the flow and are used to normalize profiles of statistical quantities.

Figures 1 show normalized profiles of the main statistical quantities for $Re = 30,000$ and $r = 0.15$. The results of the other configurations (Re, r) and the results of Bradbury (1965) for the same configuration (not shown here) present the same behaviours. The normalized profiles of the mean velocity $\langle u \rangle$ (figure 1 top-left) are well fitted by the Gaussian

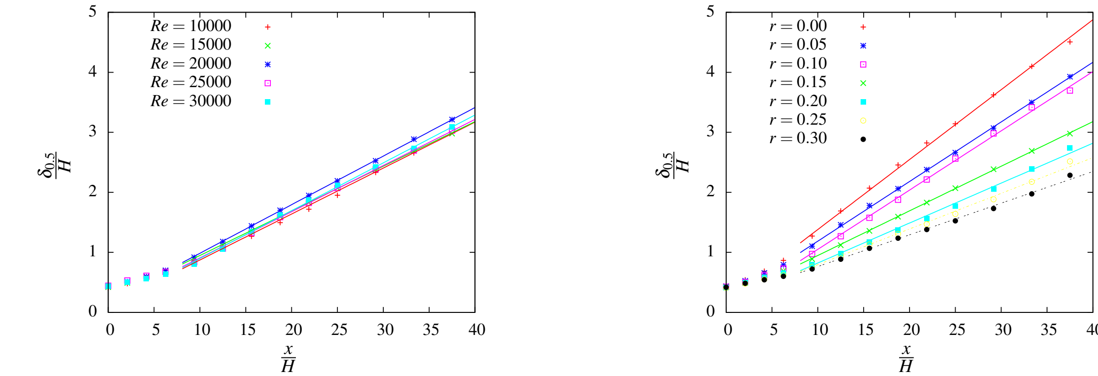

Figure 4. Streamwise variation of the velocity half-width $\delta_{0.5}$ on the centreline: left, $r = 0.15$ for various Reynold numbers; right, $Re = 15,000$ for various velocity ratios. Lines are the fitting eqn 9 to the data.

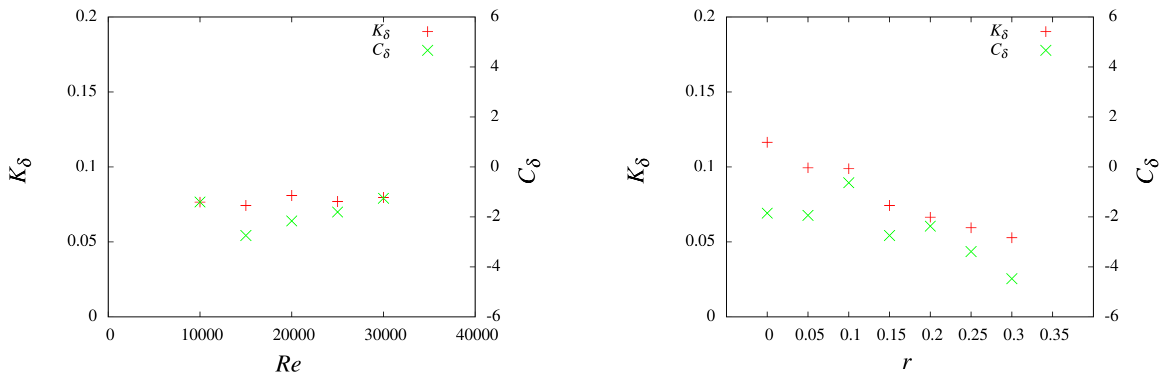

Figure 5. Jet spreading rate K_δ and virtual origin C_δ for the velocity half-width: left, $r = 0.15$; right, $Re = 15,000$.

function (eqn 7) beyond the potential core. This result agrees with the existence of a region where the velocity profiles are self-similar. The characteristic quantities of the jet estimated from these profiles are then well assessed. The normalized profile of the mean velocity $\langle v \rangle$ (figure 1 top-right) verifies the expected antisymmetric shape that can be deduced from the continuity equation for the mean flow (see Gutmark & Wygnanski (1976)). Inside the jet, the two extreme values correspond to the jet spreading due to the turbulent diffusion outward. Outside the jet, the non-zero values correspond to the entrainment velocity inward the jet due to the increase of volume flow rate Q downstream. These two effects seem to be self-similar with this scaling.

The profiles of the mean turbulent kinetic energy $k = \frac{1}{2}(\langle u'u' \rangle + \langle v'v' \rangle + \langle w'w' \rangle)$ (figure 1 bottom-left) and the Reynolds shear stress $\langle u'v' \rangle$ (figure 1 bottom-right) are respectively symmetric and antisymetric with the same extreme value on either side of the jet centreline. The well recovered shape due to the centreline symmetry emphasizes the measurement quality. These extrema occur at the location for which the mean velocity gradient of $\langle u \rangle$ present also an extremum. In others words, the energy is maximum where the energy production is also maximum. For these two turbulent quantities, the self-similar behaviour appears further downstream than for the mean velocity profiles.

Figures 2 show the mean velocity decay of $\langle u \rangle$ on the centreline at $r = 0.15$ for various Reynolds numbers and at $Re = 15,000$ for various velocity ratios. With the chosen representation, the constant velocity which can be used to define the potential core region is plotted as a constant function and the $x^{-1/2}$ decay of strong or weak jet in the fully turbulent region is plotted as an increasing linear function. In the potential core region, the length of the potential core x_p is roughly $6H$ but this value seems to depend slightly on the Reynolds number and the velocity ratio. In the fully turbulent region, the mean velocity profiles on the centreline follow a $x^{-1/2}$ decay as expected for a strong or weak jet. The centreline decay rate does not depend of the Reynolds number but decreases strongly with the velocity ratio, as for a mixing layer. The variation of the centreline mean velocity is represented as:

$$\left[\frac{(U_j - U_e)}{(\langle u \rangle_{cl} - U_e)}\right]^2 = K_u \left(\frac{x}{H} - C_u\right) \qquad (8)$$

where K_u is the slope that describes the centreline decay rate and C_u is the location of the virtual origin. Figures 3 present this centreline decay rate K_u and virtual origin C_u of the mean velocity with respect to the Reynolds numbers at $r = 0.15$ and velocity ratio at $Re = 15,000$. The strong velocity ratio depen-

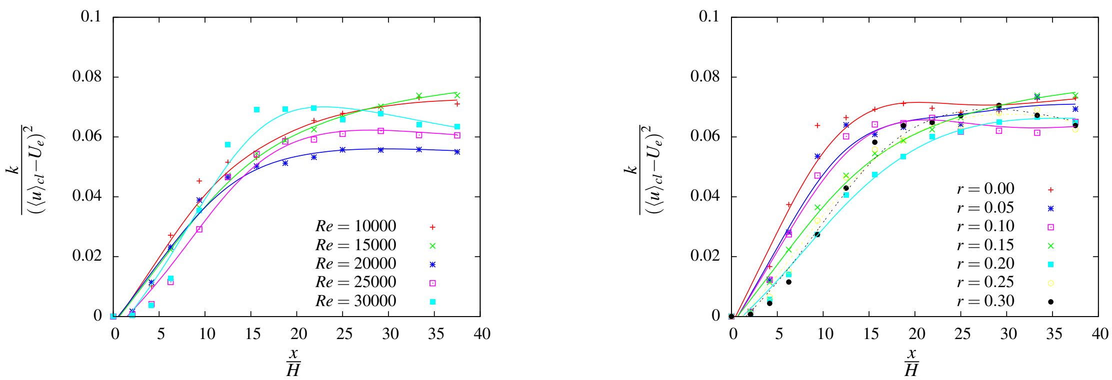

Figure 6. Evolution of mean turbulent kinematic energy k on the centreline: left, $r = 0.15$; right, $Re = 15,000$.

dence of the K_u is recovered. The behaviour of the plane jet in the fully turbulent region is independent of the upstream conditions as the nozzle geometry of boundary layer state. K_u can be easily compare with other experiments. In contrast, the virtual origins C_u depend strongly on these upstream conditions and therefore it is difficult to add comment.

Figures 4 display the streamwise variation of the velocity half-width $\delta_{0.5}$ on the centreline at $r = 0.15$ for various Reynolds numbers and at $Re = 15,000$ for various velocity ratios. In the potential core region, the variation is linear in accordance with the linear deviation of the two mixing layer outward the jet. In the self-similar region, the jet expands linearly. This result calls for a strong jet in the range of $(Re, r, x/H)$ of the present work, in accordance with the results of Bradbury (1965). This result also agrees with Everitt & Robins (1978) who observed a $x^{1/2}$ expansion only farther downstream and for higher velocity ratio. The velocity half-width of a plane jet is known to meet:

$$\left[\frac{\delta_{0.5}}{H}\right] = K_\delta \left(\frac{x}{H} - C_\delta\right) \tag{9}$$

where K_δ is the slope which describes a linear expansion of $\delta_{0.5}$ and C_δ is the location of the virtual origin. K_δ is taken to be a measure of the jet spreading rate. Figures 5 show the jet spreading rate K_δ and virtual origin C_δ for the velocity half-width for $r = 0.15$ with various Reynolds numbers and for $Re = 15,000$ with various velocity ratios. As for the centreline decay rate K_u, the jet spreading rate K_δ decreases with the velocity ratio and seems to be Reynolds number independent.

Figures 6 displays the evolution of the mean turbulent kinematic energy k on the centreline at $r = 0.15$ for various Reynolds numbers and at $Re = 15,000$ for various velocity ratios. As x/H is increased, k normalized by the local mean velocity excess seems to grow rapidly from the exit value to a constant value in the far field. In the region of constant value, the normalized profiles of k are self-similar. For example, the normalized profiles of k are self-similar beyond $x/H \simeq 20$ for the configuration $(Re, r) = (30,000, 0.15)$ (see figure 1 bottom left). The location of the beginning of the self-similar region for the second order moments depends mainly on the velocity ratio.

CONCLUSIONS

The completed work had generated a database on the plane jet with co-flow for large range of $(Re, r, x/H)$. In the current study, we focus mainly on the first and second order moments. It appears than the plane jet behaves as a strong jet in the self-similar region explored $(x/H < 37.5)$. In this region, the centreline decay rate K_u and jet spreading rate K_δ depend slightly of the Reynolds number but strongly of the velocity ratio. Self-similarity occurs farther downstream for the turbulent flow that suggests the initial conditions have much more persistent effects on turbulence. The current work is a prior study preparing the investigation of the cold/warm plane jet developing between two co-flow with different velocity and temperature. For the future study, a new variable temperature HWA method is being developed to allow simultaneous measurement of velocity and temperature at the same point with a single wire (see Ndoye *et al.* (2010)). This new anemometer may be able to characterize the mechanisms of scalar transfer of a forced and even-mixed convection regime.

REFERENCES

Bradbury, L. J. S 1965 The structure of a self-preserving turbulent plane jet. *Journal of Fluid Mechanics* **23**, 31–64.

Everitt, K. W. & Robins, A. G. 1978 The development and structure of turbulent plane jets. *Journal of Fluid Mechanics* **88**, 563–583.

Gutmark, E. & Wygnanski, I. 1976 The planar turbulent jet. *Journal of Fluid Mechanics* **73**, 465–495.

Heskestad, G. 1965 Hot wire measurements in a plane turbulent jet. *J. Appl. Mech.* **32**, 721–734.

Le Ribault, C., Sarkar, S. & Stanley, S. A. 1999 Large eddy simulation of plane jet. *Physics of Fluids* **11** (10), 3069–3083.

Ndoye, M., Delville, J., Heitz, D. & Arroyo, G. 2010 Parameterizable Constant Temperature Anemometer, a new method for the analysis of velocity-temperature coupling in turbulent heat transfer. *Meas. Sci. Technol* **21** (7), 075401.

Rajaratnam, N. 1976 *Turbulents jet*. Amsterdam: Elsevier.

Van Der Hegge Zijnen, B.G. 1958 Measurements of the velocity distribution in a plane turbulent jet of air. *Appl. sci. Res* **A-7**, 256–276.